Diagnostic of functionality of polymer membrane – based ion selective electrodes by impedance spectroscopy†

Aleksandar Radu,*[a] Salzitsa Anastasova-Ivanova,[a] Beata Paczosa-Bator,[b] Marek Danielewski,[b] Johan Bobacka,[c] Andrzej Lewenstam[c] and Dermot Diamond*[a]

Received 17th April 2010, Accepted 26th July 2010
DOI: 10.1039/c0ay00249f

Electrochemical impedance spectroscopy (EIS) is a powerful tool for the analysis of various electrochemical systems because it allows the separation and characterization of individual kinetic processes. In this paper we investigate whether changes in the EIS characteristics can be used to distinguish between solid-state ISE membrane that have been subjected to physical damage, biofouling or leaching of active components. We conclude that with these relatively simple electronic measurements, we can effectively evaluate the functionality of the ISE membrane; *i.e.* we can predict whether the sensors are fully functional, in need for calibration or are completely non-functional. We believe this could form the basis of a simple but effective diagnostic tool for probing the condition of remotely deployed ISEs in widely distributed chemo-sensor networks (*e.g.* for environmental monitoring) and for enhancing the reliability of these devices. Our ultimate goal is to implement such tools in place of conventional approaches to ISE testing like calibration with standard solutions, which require the integration of complex and costly fluidics.

Introduction

The realization that the limit of detection of simple potentiometric sensors, commonly referred to as ion selective electrodes (ISEs), can be lowered to part-per-trillion (ppt) levels[1] has opened new possible fields of application. From a technique that was almost exclusively applied to the analysis of blood electrolytes, ISEs are today finding new applications in environmental monitoring,[2] immunoanalysis,[3] DNA analysis,[4] health and exercise science.[5]

New applications carry new challenges and opportunities. For example, health diagnostic devices are becoming simpler and often integrated within clothing[5] or adjusted for use at home or in the doctor's office. Devices for environmental monitoring are increasingly integrated with autonomous communications platforms (often called motes) and deployed within wireless sensing networks. The simplicity and reliability of sensors, and the cost per sensing unit are critical for the realisation of these new applications as the sensors may be handled by non-professionals, or their operation could be completely autonomous. While reducing the need for calibration may address the issues of simplicity and cost, it may significantly affect the reliability of sensors. Therefore, development of simple but effective diagnostic tests for determining sensor condition and functionality emerges as a key research topic in the development of functioning systems.

Electronic signals are commonly used to probe the condition of many types of physical sensors (*e.g.* temperature, conductivity, accelerometers *etc.*). In chemical sensing, resistance measurements have been used to track the leaching of vital membrane components such as ligands and anion exchangers, and thresholds identified that were correlated with device malfunction.[6]

Since the response of ISEs depends on the activity of ions of interest at the sample/membrane interface, changes in the membrane surface are likely to influence the device's response characteristics. For example, deployed sensors can very easily come into contact with debris present in the water and sensor surfaces may get physically damaged. Perhaps one of the most significant factors influencing the performance of *in situ* deployed sensors is biofouling. Every year millions of Euros are spent in active sensor maintenance and in research on combating biofouling. Leaching of membrane components affects the bulk composition of the sensing membrane, and this can affect response characteristics like sensitivity, limit of detection, selectivity and baseline drift. Simple electronic diagnostic tests that can probe the surface and bulk membrane condition would therefore greatly assist in the effective operation and maintenance of deployed autonomous systems.

In this paper, we suggest that electrochemical impedance spectroscopy (EIS) could provide important information on the membrane condition and sensor functionality. Having such information would allow introduction of relatively simple but powerful self-diagnostics for remotely deployed chemical sensors and enable characterization of sensors' condition without using classical calibration methods. This could reduce the regularity at which calibrations are performed, using EIS diagnostic between calibration sessions, thus significantly reducing the amount of standards and reagents required to keep the device functioning.

Perhaps in the future, with a combination of known degradation behaviour, electronic diagnostics and better

[a]*CLARITY: The Centre for Sensor Web Technologies, National Centre for Sensor Research, School of Chemical Sciences, Dublin City University, Dublin 9, Ireland*
[b]*University of Science and Technology, AGH, 30-059 Krakow, Poland*
[c]*Abo Akademi University, Process Chemistry Centre, c/o Laboratory of Analytical Chemistry, Biskopsgatan 8, FI-20500 Turku-Abo, Finland*
† Electronic supplementary information (ESI) available: Additional data. See DOI: 10.1039/c0ay00249f

knowledge/control of the sensor biological interface, the need for classical calibration could be removed entirely, leading to chemical sensing systems that are significantly simpler and lower cost than existing devices. EIS is today an important tool for characterization of interfacial properties of PVC-based ISEs.[7] EIS was previously used to investigate the influence of membrane components (ion exchangers,[8] ionophores,[9] plasticizers[10,11]) and to understand adsorption and fouling mechanism of proteins and surfactants.[12–15]

In this work, we utilize the potential of EIS to elucidate both surface- and bulk- membrane related phenomena in ISEs under conditions likely to affect their functionality in real-life situations. Examples include the effect of physical damage to the membrane, exposure to natural waters containing high bacteria levels and simulated leaching of membrane components. Our goal is to identify parameters that are correlated with changes in the membrane surface and/or bulk state which will affect sensor functionality. This will assist in the design of simplified electric circuitry that can probe the functionality of sensors and monitor critical thresholds beyond which the sensor performance is no longer analytically acceptable.

Experimental

Reagents

For membrane preparation, high molecular weight poly(vinylchloride) (PVC), bis(2-ethylhexyl) sebacate (DOS), 2-nitrophenyl octyl ether (NPOE), tetrahydrofuran (THF), *tert*-butylcalix[4]arene-tetrakis(N,N-dimethylthioacetamide) (ionophore Pb IV), sodium tetrakis-[3,5-bis(trifluoromethyl)phenyl] borate (NaTFPB) and poly(3-octylthiophene) (regiorandom) were Selectophore grade from Sigma. Milli-Q reagent-grade deionised water was used to make all sample solutions.

Solid-contact ion-selective electrodes

The miniaturized, all-solid-contact ISEs (SCISEs) were prepared by screen printing using DEK 248 printer. Ag-based ink was first used to print the contact wire onto the base. At the inner end of the silver wire, carbon-based ink was used to print the electrode. An insulator was then printed on top covering everything but a small area of the electrode and the outer end of the wire. Poly(3-octylthiophene-2,5 diyl) (POT) was used as intermediate layer as described previously.[16] The POT layer was prepared from chloroform solution (2.5 mM) and drop-cast on the carbon ink-based contact. Four layers of the polymer were cast, and the solvent was allowed to evaporate between each layer. The cocktail for the Pb^{2+}-selective membrane was prepared by dissolving 5 mmol/kg NaTFPB, 15 mmol/kg PbIV, 32 wt% PVC, and 66 wt% of DOS in 3 mL THF. The resulting solution was drop cast onto the previously deposited and dried POT layer until an ion-selective membrane (ISM) of approximately 0.40 mm thickness was obtained. The Ag/C/POT/ISM electrodes prepared in this manner were then conditioned overnight in 10^{-3} M $Pb(NO_3)_2$. Prior to recording the potentiometric calibration curves, electrodes were further conditioned for 24 h in a solution of 10^{-8} M $Pb(NO_3)_2$ adjusted to pH 4 with HNO_3.

Pb^{2+}-selective liquid contact (LCISEs) electrodes were prepared by dissolving 5 mmol/kg NaTFPB, 12 mmol/kg PbIV, 32 wt% PVC, and 66 wt% of DOS in 3 mL THF. The resulting solution was cast into a 22 mm i.d. glass ring fixed to a glass plate. After THF evaporation, a flexible membrane of ~200 μm thickness was obtained. PVC/THF adhesive was used to attach 6 mm diameter disks of this ISE membrane to the distal end of a 2 cm length of PVC tubing (3.2 mm i.d.). The PVC tubing was then attached to a 1 ml pipette tip and filled with an inner solution of 1×10^{-4} M $Pb(NO_3)_2$ and 1×10^{-3} M NTA adjusted to pH = 7. A second pipette tip with a sponge plug at its narrow end was attached to the first pipette tip and filled with 1×10^{-3} M KCl. The electrodes were conditioned for 1 day in 1 mM $Pb(NO_3)_2$ solution and second day in a solution of 10^{-8} M $Pb(NO_3)_2$ adjusted to pH 4 with HNO_3.

Sample preparation

Physically damaged SCISEs were prepared either by puncturing the membrane using a sharp object inflicting various levels of damage or by cutting the membranes inflicting damage to the membrane surface and even cutting the entire piece of the membrane (in the case of all-solid-contact ISEs). The extent of damage of LCISEs either by puncturing and/or cutting resulted in slow but steady loss of inner solution.

Biofouling of ISEs was studied by exposing the electrodes to fresh samples of water obtained from a local river (The Tolka) flowing through the city of Dublin, Ireland. Water was collected, brought into the laboratory and transferred in several interconnected reservoirs. The water was kept at constant temperature (20 °C) and under the constant flow of O_2. Electrodes were immersed in the water and kept for 1, 2, 4 and 7 days.

Leaching of membrane components was mimicked by preparing ISEs without ionic sites (referred to as "ion exchanger-free"), without ionophore ("ionopore-free") or without both ionic sites and ionophore ("blank"). The composition of these membranes was, respectively:

– *Ionic sites-free ISE* 15 mmol/kg PbIV, 33 wt% PVC, and 66 wt% of DOS in 3 mL THF.

– *Ionophore-free ISE* 5 mmol/kg NaTFPB, 33 wt% PVC, and 66 wt% of DOS in 3 mL THF.

– *Blank ISE* solution of 34 wt% PVC, and 66 wt% of DOS in 3 mL THF.

Slime test – glyococalyx production of bacteria

ISEs were immersed in Carnoy's solution (absolute ethanol, chloroform, glacial acetic acid; 6 : 3 : 1), placed in a centrifuge tube and left for a 1 h period. The Carnoy's solution was then decanted off and the ISEs were washed three times with Milli-Q water. Toluiende blue (0.1%) was added to ISEs and left for another 1 hour period. The dye was then decanted off and ISEs were washed 3 times with Milli-Q water followed by the addition of sodium hydroxide (0.2 M) and heating at 80 °C for another 1 hour period. The samples were allowed to cool and analysed for bacteria production by measuring the absorbance of the coloured solution at 590 nm.

Potentiometric measurements

Potentiometric measurements were performed at room temperature (21 °C) using a 16-channel electrode monitor (Dawson

Labs). EMF measurements were conducted in stirring solutions using a Metrohm 728 stirring plate using a Ag/AgCl double junction reference electrode (Metrohm, 6.0729.100) with 3 M KCl internal filling solution and 1 M LiOAc as bridge electrolyte. Measured values were corrected for liquid-junction potentials using the Henderson equation[17] and ion activities were calculated according to the Debye–Hückel approximation.[18]

Note that all potentiometric measurements presented in the following figures were done using at least three electrodes. For clarity reasons, data are presented for one representative electrode.

Electrochemical impedance spectroscopy measurements

EIS studies were undertaken using a CHI660C Potentiostat from IJ Cambria Scientific Ltd. Because of the low conductivity of the polymer membranes, all EIS spectra were collected using four-point averaging statistics to increase the signal-to-noise ratio (excitation potential = 100 mV root-mean-square (rms), frequency range 100 kHz to 1 mHz). A conventional three-electrode cell contained in a 10^{-3} M solution of $Pb(NO_3)_2$ was used, with all solutions maintained at 20 ± 1 °C for all measurements. Both solid-state and liquid-state Pb-selective ISEs were used as working electrodes, in combination with a platinum counter electrode and a silver/silver chloride double-junction reference electrode. Equivalent circuits used to model the impedance spectra are shown in Fig. 1.

Note that EIS measurements for electrodes which were used for studying biofouling and leaching of membrane components were done on at least three electrodes while for clarity reasons data are presented for one representative electrode. In the case of physically damaged ISEs due to the poor reproducibility of the extent of damage inflicted by puncturing and cutting, measurements are done on one ISE.

Results

1. Physical damage. The ISE membranes were deliberately damaged by puncturing and cutting in an attempt to simulate possible situations occurring in real deployments and to estimate the effect of such damage on their functionality. Two types of ISEs were used: LCISEs and SCISEs. As expected, LCISEs were prone to complete loss of functionality when the membrane was damaged. Inflicting damage on the membrane enables the contact to be established between the inner solution and the sample resulting in total collapse in response characteristics, as shown in ESI (Fig. S1).†

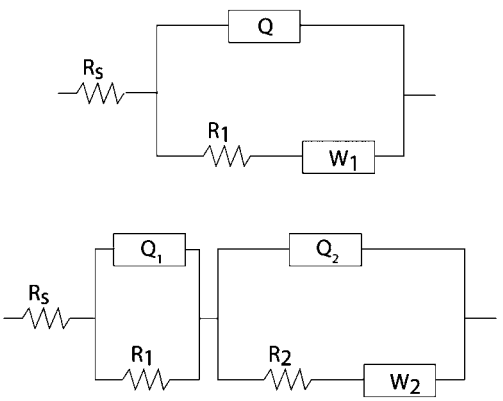

Fig. 1 Equivalent circuits used to fit EIS data in the case of one resistive layer (top) and two resistive layers (bottom). Circuit elements are defined as follows: R_s is the solution resistance, R_1 and R_2 are resistance elements of each individual layer, Q_1 and Q_2 are constant phase elements and W is Warburg impedance.

On the other hand, SCISEs were expected to be more robust since they do not have any liquid phases. Fig. 2 depicts scanning electron microscopy (SEM) images of damaged SCISE membranes. The extent of damage was varied from no damage (Fig. 2A) to single (Fig. 2B) and multiple holes produced by puncturing the membrane with sharp object (Fig. 2C) and to single (Fig. 2D) and multiple (Fig. 2E) cuts. Please note different magnification in cases C and E (1 mm and 2 mm respectively) relative to corresponding B and D (500 μm) which is chosen to present damage rather than the extent of each piercing and/or cut.

Fig. 3 depicts potentiometric (left) and EIS (right) characterization of physically damaged SCISEs in comparison to the so called "optimised" electrode (electrode #1 – undamaged and properly conditioned). Potentiometrically, the latter shows a detection limit of $log_{pb,LOD} = -8.2$. This is close to that predicted by theory[19] (please see ESI†) under the experimental conditions employed. Characterization of SCISEs was done in accordance with recommendations for solid-contact ISEs from Lindner *et al.* with special consideration of the so called "water layer test".[16] Detailed description of theoretical calculations of detection limit and protocol for "water layer test" is given in ESI.†

In contrast with the LCISEs, the response of the SCISEs is quite striking. Even upon removing half of the membrane (Fig. 3 left, dashed line – electrode #5) and leaving the POT layer only partly covered with ion-selective membrane, the SCISE continued to function and exhibited a Nernstian response and detection limit in μM range. Please note that due to the irreproducibility of the extent of damage we show potentiometric responses of only the two most extreme cases – no damage (optimised ISE) and the case in which the entire half of the membrane is removed. The observed retention of the potentiometric functionality is very surprising. In the system containing ionically conductive membrane (ISE) coexisting with mixed electronic and ionic conductive membrane (POT) exposed to the same solution it is expected that the exposed POT layer would significantly influence the response characteristics (sensitivity, selectivity, detection limit) of the electrode. Since it has been demonstrated that incorporation of ionophore and ionic sites into the conductive polymer POT can result in an ion-selective membrane behaviour[20] diffusion of membrane components into conductive polymer layer thereby rendering it potentiometrically responsive should not be ruled out.

For our study however, the fact that severely damaged SCISEs can continue to provide potentiometric information even when quite severely damaged, is an important outcome, even with the loss of response at concentrations below 10^{-6} M. In other words, an SCISE in an autonomous sensing device may appear to be still properly functioning if subjected to a conventional calibration routine using standard solutions above 10^{-6} M. These results suggest that the simple electronic EIS measurements may in fact

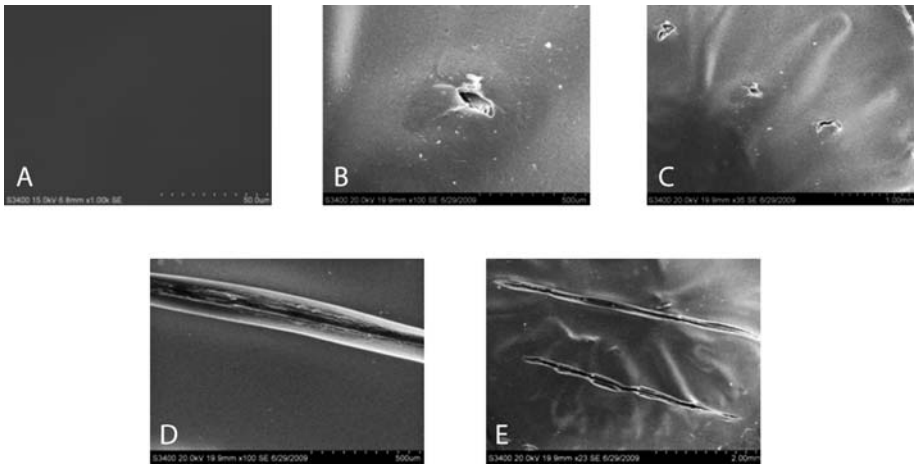

Fig. 2 SEM micrographs of the following POT/ISM films: **A** optimised (as prepared) at 50 μm magnification; **B** pierced electrode (one time) at 500 μm magnification; **C** pierced electrode (three times) at 1 mm magnification; **D** cut electrode (one time) at 500 μm magnification; **E** cut electrode (two times) at 2 mm magnification.

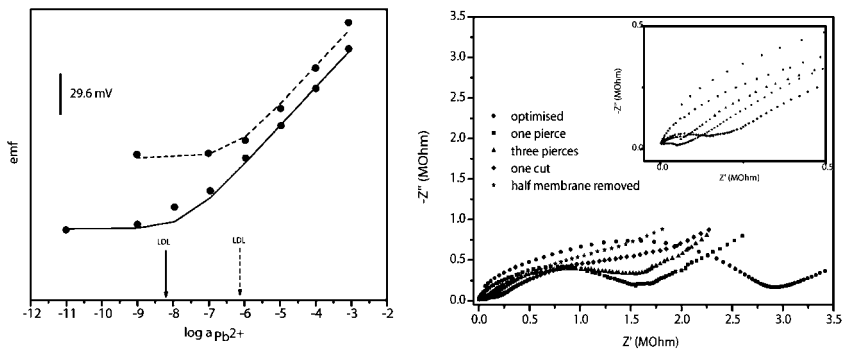

Fig. 3 (Left) Potentiometric response of optimised (solid line) and severely damaged Pb^{2+}-selective electrode (dashed line). (Right) EIS spectra of optimised (circle) and damaged Pb^{2+}-selective electrode (extent of damaged is noted on the figure). Inset depicts EIS spectra in the range of 0.5 MOhm.

be more informative than much more complex fluidic-based calibrations for characterising sensor functionality.

Fig. 3 right depicts EIS characterization given in the form of Nyquist plots of physically damaged ISEs. Starting from the "optimised" electrode (full circles), we observe a typical semi-circle related to the bulk resistance of the membrane in parallel with the geometric capacitance of the membrane. The semicircle is followed by a Warburg impedance part. Values for bulk membrane resistance, Warburg impedance and constant phase element expressed as

$$Q = \frac{1}{Y_0(j\omega)^n}$$

where Y_0 is a frequency independent pre-exponential factor, ω is frequency, j is the imaginary unit and n is the exponent which defines character of the frequency dependence and can take values of $1 \leq n \leq 0$. Values given in Table 1 are obtained by fitting experimental data using equivalent circuits given in Fig. 1.

Upon puncturing and cutting, the damaged ISM membrane facilitates diffusion of ions to the POT layer. Physical damage gives a low-resistance pathway for ion diffusion which is observed as a decrease of the Warburg impedance values from 1×10^{-5} Ohm for electrode #1 and #2 to 6×10^{-6} Ohm for electrode #3, 3×10^{-6} Ohm for electrode #4, to 1×10^{-6} Ohm for electrode #5 where half of the ion-selective membrane is removed (see Table 1 physical damage sector). In addition, as the damage becomes more severe, the influence of the underlying POT layer and POT/solution interface becomes more obvious through the appearance of two semicircles in electrodes #3, #4 and #5. In these cases, equivalent circuit B from Fig. 1 was used for fitting experimental data. The impedance spectrum of electrode #5 is very similar to the GC/POT electrode reported earlier where Bobacka *et al.* argue that the high frequency semicircle gives bulk resistance (in this work given as R_1) and geometric capacitance (C_2) of the POT membrane.[20] The low-frequency semicircle can be interpreted as the charge-transfer resistance (R_2) and double-layer capacitance originating from the POT/solution interface.[20] Arising from the latter, physical damage of the membrane strongly influences the low frequency region of the impedance.

2. Biofouling. The impact of biofouling on the response function of ISEs is shown in Fig. 4 left, while EIS characterisation is shown on the right.

ISEs were exposed to water from river Tolka that flows through Dublin, Ireland, according to protocol described in

Table 1 Equivalent circuit element values for optimised Pb^{2+}-selective electrode and electrodes that were exposed to physical damage, biofouling and leaching

	electrode number	electrode description	Rs	R1	n1	Yo1	W1	R2	n2	Yo2	W2
	1	optimised	500	3.0E + 06	0.6	5.0E-08	1.0E-G5				
physical damage	2	one hole	500	1.6E + 06	0.6	1.0E-07	1.0E-05				
	3	three hole	500	6.0E + 04	0.7	1.0E-08		1.5E + 06	0.6	2-0E-07	6.0E-06
	4	two cuts	500	1.5E + 05	0.7	5.0E-09		1.8E + 06	0.55	2.5E-07	3.0E-06
	5	half ISE removed	500	7.0E + 04	0.7	1.0E-09		1.8E + 06	0.55	2.0E-07	1.0E-06
biofouling	6	1 day	500		0.6	5.0E-09		2.0E + 06	0.65	1-0E-08	5.0E-06
	7	2 day	500	5.0E + 05	0.65	5.0E-09		1.1E + 06	0.7	1.0E-08	7.0E-06
	8	4 day	500	1.4E + 06	0.62	3.0E-08	1.0E-05				
	9	7 day	500	1.2E + 06	0.6	4.0E-08	1.0E-05				
leaching	10	ionophore-free	500	1.6E + 06	0.75	1.0E-08	1.0E-05				
	11	ion exchanger-free	500	5.5E + 07	0.63	1.0E-08	1.0E-05				
	12	blank	500	9.0E + 07	0.72	1.0E-08	1.0E-05				

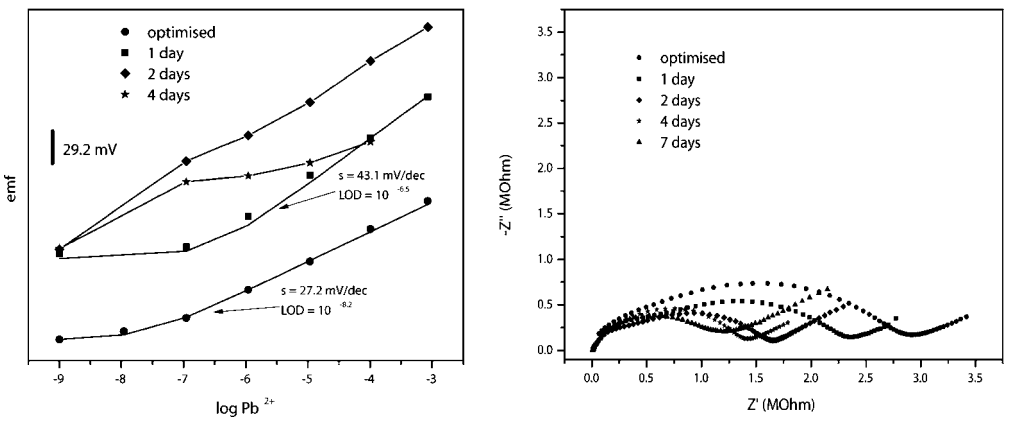

Fig. 4 (Left) Potentiometric responses of Pb^{2+}-selective electrode – optimised (circles), exposed to natural river water for 1 day (squares), 2 days (diamonds) and 4 days (stars). Note that the responses of the latter 3 electrodes were normalized at 10^{-9} M in order to point out differences in response slopes. (Right) EIS spectra of Pb^{2+}-selective electrode (circles) and electrodes that were exposed to natural river water for 1 day (squares), 2 days (diamonds), 4 days (stars) and 7 days (triangles).

Experimental. Tolka river is known to be highly microbiologically polluted containing total coliforms and e. coli that are far above EU and National Bathing Water Limits.[21] The potentiometric response of Pb^{2+}-ISEs that were exposed to bacteria-rich natural water for only one day (squares in Fig. 4 left) deviated significantly from the optimised ISE response (circles). The detection limit increased by ~1.7 orders of magnitude while the slope changed from nernstian (27.2 mV/decade) in electrode #1 (optimised) to supernernstian (43.1 mV/decade) in electrode #6 (fouled for 1 day). Further exposure to bacteria-rich waters resulted in electrodes having supernernstian slope (38.7 mV/decade) in the range from 10^{-7} M to 10^{-3} M and demonstrating severe drifts when exposed to initial calibration solution (Pb^{2+}-free and pH = 4). Please note that the point at 10^{-9} M at Fig. 4 left does not represent true steady state condition but rather a point where drifts were reduced to a value ~2 mV/min achieved after ~1 h of equilibration time. It therefore gives a false impression of nanomolar detection limit. Similar drifts were observed with electrodes exposed to bacteria-rich water for 4 days and Fig. S3 in ESI† depicts drifts observed in one such electrode (electrode #8). These severe initial drifts most likely originate from ill-defined aqueous diffusion layer. The layer of slime deposited by bacteria (commonly referred to as Glycocalyx which is a polysaccharide or polypeptide network that connects to the endothelium through proteoglycans and glycoproteins and where soluble molecules are incorporated[22]) most likely acts as an intermediate diffusion layer with its own ill-defined thickness (due to constant deposition of new slime by bacteria) and diffusion coefficient. This influences diffusion of lead ions at membrane/sample interface ultimately affecting the ion fluxes described with equation SEq2 in ESI.† For further discussion on ion fluxes and their influence on steady-state and real-time electrode responses please refer to the works of Ceresa *et al.*[23] and Radu *et al.*[24] respectively. In addition to drifts in the response of electrode #8 we observed almost complete loss of functionality. Some response to Pb^{2+} was observed only in millimolar range (please see response curve labelled with stars in Fig. 4 left). This rapid decline in sensitivity is quite surprising given that ISEs are commonly used in matrices that are expected to generate severe biofouling. For example, the most significant application field of ISEs is in whole blood analysis.[25] However, although immersion in blood does cause fouling of ISE membranes, almost all measurements in blood are not continuous and it is recommended that measurements last approximately 10 min, and that electrodes are cleaned after every measurement.[26] An interesting example of using ISEs in continuous measurements in natural

waters was described by Le Goff *et al.*[27] They used nitrate-selective electrodes and observed no deterioration of performance due to biofouling even after 40 days. These authors speculate that the reason for such excellent biofouling resistance was due to usage quaternary ammonium compounds as ion exchangers since they have a well-documented antimicrobial effect.[28] Since cation selective ISEs (like the Pb^{2+}-selective electrodes used in this study) do not use quaternary compounds in the membrane they therefore become prone to severe biofouling by bacteria.

The growth of the bacterial films on the sensor membranes was monitored using the so called "slime" test as explained in Experimental. Fig. 5 shows absorbance of the solution obtained by dissolution of the biofilm from the surface of ISEs. The values are normalized to the slime test value obtained for a non-biofouled ISE. It can be seen that biofilm initiation happens within one day, and the film rapidly grows with time, as demonstrated by almost 9-fold increase in absorbance of solutions originating from electrode #9 (biofouled for 7 days) compared to electrode #6 (biofouled for 1 day).

Biofilm growth was also studied using EIS. Fig. 4 (right) shows a comparison of Nyquist plots of optimised ISEs (full circles) to ones exposed to bacteria for 1 (squares), 2 (diamonds), 4 (stars) and 7 days (triangles).

In the EIS spectra, bulk membrane resistance (semicircle) and Warburg impedance regions can be clearly seen. Interestingly, the bulk resistance decreases with the growth of biofilm on the membrane surface, most likely due to membrane deterioration arising from microbial activity.[29] The deterioration can be

a) *physical* – microbial species adhere to surfaces due to the secretion of glycocalyx which infiltrates porous structures altering the size and the distribution of pores and changing the moisture content and thermal transfer behaviour;

b) *chemical* – bacterial flora use inorganic and organic matter as carbon, energy and electron sources which can interfere with electrode function; and,

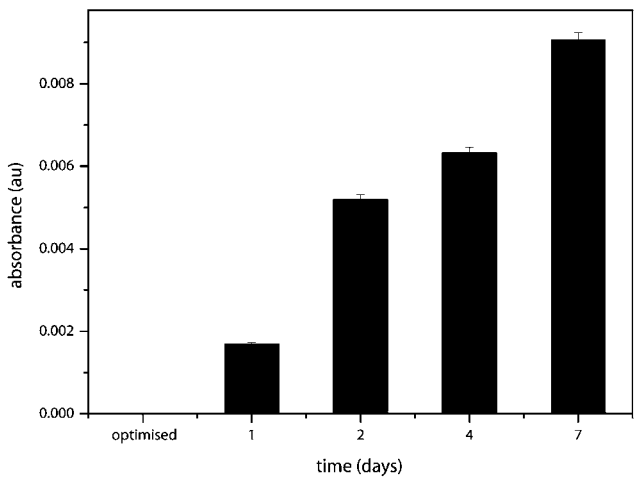

Fig. 5 Amount of slime deposited by bacteria on ISEs measured according to the protocol described in Experimental. All results were normalised on optimised electrode (electrode that was not exposed to bacteria-rich waters). Measurements are done in triplicate and with resulting standard deviation of ~2% presented as error bars.

c) *enzymatic* – some bacterial enzymes involved in biodeterioration use cations present in the material matrix as cofactors, which can affect the overall ion content and extraction behaviour of the sensing membrane or film.[30]

In addition, it has been recently demonstrated that microorganisms can significantly enhance the kinetics of electron transfer reactions, resulting in a decrease in bulk resistance.[31] Interestingly, after the exposure of biofouled membranes to deionized water for several days, we observed an increase in bulk resistance to levels similar to the original non-fouled electrode (data not shown). It is likely that upon exposure of electrodes to clean water, the biofilm and interfering byproducts are removed from the membrane surface and the original membrane resistance is restored.

In addition, Nyquist plots very clearly demonstrate two semicircles even after one and after two days exposure. According to the discussion above, the biofilm behaves as an additional layer through which ions have to diffuse and EIS spectra demonstrating two semi-circles indicate that electrode is coated with two membrane layers (ion-selective membrane and biofilm). Such spectra can be effectively modelled with an additional resistor and capacitor in the equivalent circuit. Therefore, the equivalent circuit depicted in Fig. 1 (bottom) was used to model the behaviour of this system.[31] Interestingly, the second semicircle disappeared in electrode #8 (exposed for 4 days to bacteria-rich water). Disappearance of the second semicircle indicates the existence of only one diffusion layer. We believe that at this stage the biofilm has penetrated the ion-selective membrane and modified its bulk. This effectively means that electrode is coated with only one layer (ion-selective membrane) albeit with modified bulk properties due to penetration of biofilm. This situation therefore requires that EIS spectrum is modelled using the simple one semicircle-based equivalent circuit as depicted in Fig. 1 (top). Data obtained from the modelling studies are given in Table 1. The fact that the glycocalyx layer strongly influences the diffusion of ions through the film is supported by the change in Warburg impedance in the case of electrode biofouled for one and for two days from 5×10^{-6} Ohm to 7×10^{-6} Ohm respectively.

3. Loss of the membrane components. Loss of membrane components through leaching and/or decomposition can lead to a drastic collapse of response function in sensing systems that are deployed on a long-term basis.

For simplicity, we consider only the complete loss of ionophore and/or ion exchanger to observe the most extreme (limiting) case. In this study, our goal is to find whether electrical parameters can be used to describe the *functionality of the sensor.* Fig. 6 depicts potentiometric and EIS characterization of optimised ISEs (electrode #1 in Table 1) compared with membranes that are ionophore-free (electrode #10), ion-exchanger free (electrode #11) and both ionophore and ion-exchanger free (blank, electrode #12).

In the case of "ion exchanger-free" ISEs represented by electrode #10, the response to the ion of interest (Pb^{2+} in our case) is determined by the ionophore and impurities present in the membrane. While the functionality is preserved, the detection limit corresponds to conventional, unoptimised electrodes (*i.e.* in the order of μM as shown in Fig. 6 left dashed line). On the other

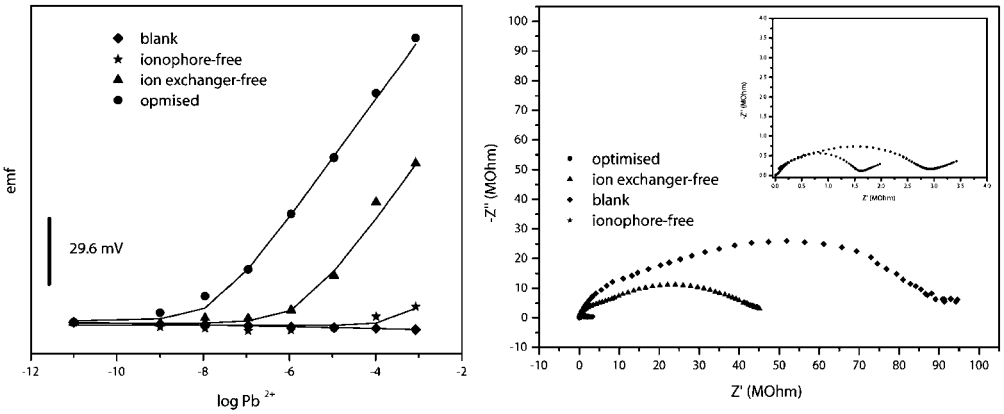

Fig. 6 (Left) Potentiometric response of optimised ISE (electrode #1, circles), ionophore-free (electrode #10, stars), ion exchanger-free (electrode #11, triangles) and blank (electrode #12, diamonds). (Right) EIS spectra of four used ISEs with the same symbols as in the Fig. 6 left. Inset depicts EIS spectra of optimised and ionophore-free ISEs.

hand, the response of "ionophore-free" electrodes is dictated by the lipophilicity of the ions of interest. This membrane will be more selective for more lipophilic, larger cations with low charge density, and less responsive to multivalent ions. This is very apparent in the minimal response to Pb^{2+} obtained (response depicted with star symbols in Fig. 6 left). As would be expected, the "blank" membrane shows a total lack of response as it contains no active components (response depicted with diamond symbols in Fig. 6 left).

Fig. 6 right shows EIS spectra for the same sets of ISEs. The inset depicts EIS spectra of electrodes #1 and #10 (optimised and ionophore-free respectively) limited to the region of <4 MOhm. In the case of electrode #10 the charge carrier is the ion exchanger (NaTFPB) within the membrane. The bulk resistance of 1.6×10^6 MOhm is smaller than in the case of optimised ISEs (3.0×10^6 MOhm) that contains the same amount of ion exchanger. However, in the latter case approximately 42% of the TFPB's counterions are replaced by the Pb-ionophore complex. The mobility of this complex is lower than uncomplexed (free) Pb^{2+} and results in higher bulk resistance of optimised ISEs.[32] On the other hand, the bulk membrane resistance of electrode #11 membranes depends only on the amount of Pb^{2+}-ionophore complex and the amount of impurities as the main charge carriers, and it is therefore higher than that of electrode #1 (5.5×10^7 Ohm). Finally, electrode #12 has the lowest concentration of charge carriers (effectively only the impurities in the components) and they therefore have the highest resistance (9.0×10^7 Ohm).

Implications

The ability to quickly and simply diagnose the functionality of ISE-based sensing systemss *without classical calibration* (*i.e.* avoiding or reducing the need for calibration, and associated solutions, waste storage, pumps, valves) could markedly simplify their fabrication and operation. Using EIS, it may be possible to identify processes happening both on the surface (physical damage and biofouling) and in the bulk of the membrane (leaching of the components and biofouling) that have a strong influence on the functionality of the sensors. Furthermore, careful analysis of the EIS Bode plots presented in Fig. 7 A, B, and C suggests that it is possible to identify optimal parameters of a simple AC electrical signal that could be used to evaluate sensor functionality.

For example, designing a circuitry for generation of AC signal using for example excitation signal of 100 mV (as described in Experimental) and a single frequency, one can observe a change in impedance as a function of sensor's functionality. Frequency window that could be used is quite wide and in Fig. 7 A, B, C we highlight an approximate possible range of 0.5–50 Hz. Fig. 7 D, E, and F depicts impedance on chosen frequency of 1 Hz for each of the three hereby studied factors. Inset in Fig. 7 F highlights the impedance of optimised electrode (electrode #1) and ionophore-free electrode (electrode #10).

The most significant implication of Fig. 7 lays in the facts that impedance measured at 1 Hz is reduced if surface of the membrane is either damaged (Fig. 7D), covered with biofilm (Fig. 7E) or components leached out from the membrane (Fig. 7F). However, all these three processes happen on a highly different time scale. Namely, physical damage is highly random and sudden, while the formation of the biofilm and ionophore leaching are continuous processes occurring at greatly different time scales. For example, leaching of ionophore and/or ionic sites is a very slow process occurring in the order of months[33,34] while the formation of biofilm happens in the order of days, as seen above.

Furthermore, apart from striving to the change in the composition of membrane components and/or surface (for example to include bactericide agents[35]) the fact that biofilm is getting reduced by bathing in a bacteria-free solution has important implications in design of housing for ISEs as detectors in a sensing device. To avoid both physical damage and prolonged exposure to bacteria, ISEs should be enclosed in a microfluidic chip. This would enable short term exposure to the sample followed by bathing in conditioning solution (bacteria-free) to increase the life time of the sensor. While it is possible to imagine that switching between the sample and bathing solution would require an additional pump, it is important to note that the work in our group also includes development of light-controlled valves.[36] Therefore a chip using simple light emitting diodes (LEDs) instead of a classical pump for the sample/bathing solution flow control could be envisioned.

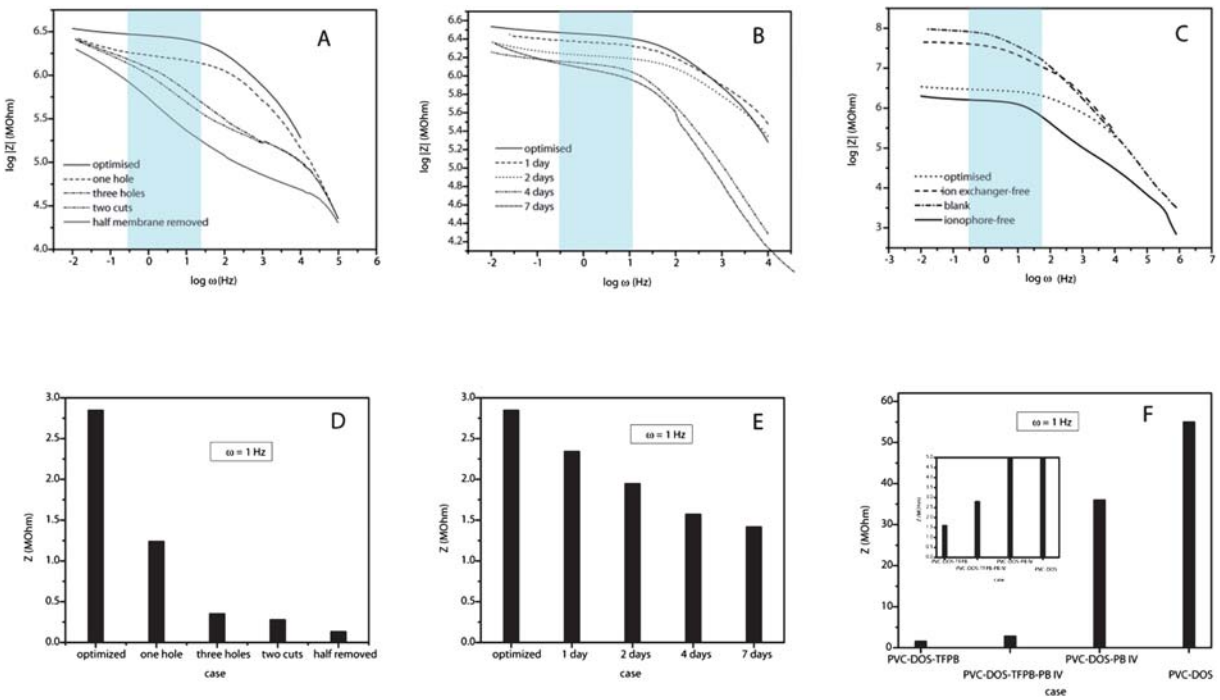

Fig. 7 (Top) Bode plot of impedance as a function of frequency. Highlighted region denotes frequency at which large changes of impedance can be observed for each of the three hereby studied factors (A-physical damage, B-biofouling, C-leaching of the components) influencing sensor's functionality. (Bottom) Impedance change at a chosen frequency from the highlighted region (1 Hz) for the three factors (D-physical damage, E-biofouling, F-leaching of the components). Inset in F depicts impedance in the range of <5MOhm to highlight impedances of optimised electrode (electrode #1) and ionophore-free electrode (electrode #10).

Considering all of the above, a microfluidic chip integrating ISEs with a simple circuitry within the sensing device using AC of certain amplitude and frequency (for example 100 mV and 1 Hz as used in this work) can be used as a very simple diagnostic tool for sensors' functionality. Periodically checking the impedance (*e.g.* once a day) it would be possible to obtain valuable information on sensors' functionality. For example, whether sensors were biofouled, damaged or components leached out hence implying the loss of optimal sensor performance. Based on obtained information, a built-in local intelligence is then able to make a decision on whether the calibration is necessary under the current state of the sensor. Consequently, slight increase in electronic and software sophistication should significantly reduce the size and more importantly the cost of device operation and maintenance through reducing/eliminating the need for bulky and expensive storage, and energy needs.

Acknowledgements

This work is supported by Enterprise Ireland (grant 07/RFP/MASF812), the Finnish Funding Agency for Technology and Innovation (Tekes grant 2084/31/06) and the National Centre for Research and Development (grant DWM/232/MATERA/2006) which are part of the EU MATERA ERA-NET initiative. The authors would also like to thank Science Foundation Ireland (grant 07/CE/I1147 and NAP210) for financial support. AR is grateful to DCU for a Research Career Start Fellowship and Research Fellowship.

References

1 E. Bakker and E. Pretsch, *TrAC, Trends Anal. Chem.*, 2008, **27**, 612–618.
2 V. I. Slaveykova, K. J. Wilkinson, A. Ceresa and E. Pretsch, *Environ. Sci. Technol.*, 2003, **37**, 1114–1121.
3 J. Szucs, E. Pretsch and R. E. Gyurcsanyi, *Analyst*, 2009, **134**, 1601–1607.
4 A. Numnuam, K. Y. Chumbimuni-Torres, Y. Xiang, R. Bash, P. Thavarungkul, P. Kanatharana, E. Pretsch, J. Wang and E. Bakker, *J. Am. Chem. Soc.*, 2008, **130**, 410.
5 D. Morris, S. Coyle, Y. Z. Wu, K. T. Lau, G. Wallace and D. Diamond, *Sens. Actuators, B*, 2009, **139**, 231–236.
6 D. Diamond and F. Regan, *Electroanalysis*, 1990, **2**, 113–117.
7 B. Pejcic and R. De Marco, *Electrochim. Acta*, 2006, **51**, 6217–6229.
8 A. Schwake, K. Cammann, A. L. Smirnova, S. S. Levitchev, V. L. Khitrova, A. L. Grekovich and Y. G. Vlasov, *Anal. Chim. Acta*, 1999, **393**, 19–28.
9 A. Lisowska-Oleksiak, U. Lesinska, A. P. Nowak and M. Bochenska, *Electrochim. Acta*, 2006, **51**, 2120–2128.
10 A. Legin, S. Makarychev-Mikhailov, D. Kirsanov, J. Mortensen and U. Vlasov, *Anal. Chim. Acta*, 2004, **514**, 107–113.
11 A. Legin, S. Makarychev-Mikhailov, J. Mortensen and Y. Vlasov, *Electrochim. Acta*, 2004, **49**, 5203–5207.
12 L. Muslinkina and E. Pretsch, *Chem. Commun.*, 2004, 1218–1219.
13 L. Muslinkina and E. Pretsch, *Electroanalysis*, 2004, **16**, 1569–1575.
14 Q. S. Ye, Z. Keresztes and G. Horvai, *Electroanalysis*, 1999, **11**, 729–734.
15 Q. S. Ye, A. Vincze, G. Horvai and F. A. M. Leermakers, *Electrochim. Acta*, 1998, **44**, 125–132.
16 E. Lindner and R. E. Gyurcsanyi, *J. Solid State Electrochem.*, 2009, **13**, 51–68.
17 L. J. Henderson, *J. Biol. Chem.*, 1921, **46**, 411.
18 P. Debye and E. Huckel, *Physik Z.*, 1923, **24**, 185–206.
19 A. Ceresa, E. Bakker, B. Hattendorf, D. Gunther and E. Pretsch, *Anal. Chem.*, 2001, **73**, 343–351.

20 J. Bobacka, A. Ivaska and A. Lewenstam, *Anal. Chim. Acta*, 1999, **385**, 195–202.
21 Final Environmental Report (water), Dublin Regional Authority, 2006, www.dra.ie/PDF/06_FINAL_ENVIRONMENTAL_REPORT_water.pdf.
22 S. Reitsma, D. W. Slaaf, H. Vink, Mamj van Zandvoort and Mgao Egbrink, *Pfluegers Arch.*, 2007, **454**, 345–359.
23 A. Ceresa, A. Radu, S. Peper, E. Bakker and E. Pretsch, *Anal. Chem.*, 2002, **74**, 4027–4036.
24 A. Radu, A. J. Meir and E. Bakker, *Anal. Chem.*, 2004, **76**, 6402–6409.
25 P. Anker, E. Wieland, D. Ammann, R. E. Dohner, R. Asper and W. Simon, *Anal. Chem.*, 1981, **53**, 1970–1974.
26 E. Kissa, *Clinical Chemistry*, 1987, **33**, 253–255.
27 T. Le Goff, J. Braven, L. Ebdon and D. Scholefield, *J. Environ. Monit.*, 2003, **5**, 353–358.
28 G. Sykes In *Disinfection and Sterilization*, 2nd ed.; Chapman and Hall: London1965pp 369.
29 J. D. Gu, M. Roman, T. Esselman and R. Mitchell, *Int. Biodeterior. Biodegrad.*, 1998, **41**, 25–33.
30 N. Lucas, C. Bienaime, C. Belloy, M. Queneudec, F. Silvestre and J. E. Nava-Saucedo, *Chemosphere*, 2008, **73**, 429–442.
31 Federico Aulenta, Reale Priscilla, Canosa Andrea, Rossetti Simona, Panero Stefania and Majone Mauro, *Biosens. Bioelectron.*, 2010, **25**, 1796–1802.
32 T. Lindfors, J. Bobacka, A. Lewenstam and A. Ivaska, *Analyst*, 1996, **121**, 1823–1827.
33 S. Peper, Y. Qin, P. Almond, M. McKee, M. Telting-Diaz, T. Albrecht-Schmitt and E. Bakker, *Anal. Chem.*, 2003, **75**, 2131–2139.
34 P. Buhlmann, Y. Umezawa, S. Rondinini, A. Vertova, A. Pigliucci and L. Bertesago, *Anal. Chem.*, 2000, **72**, 1843–1852.
35 N. Hilal, V. Kochkodan, L. Al-Khatib and T. Levadna, *Desalination*, 2004, **167**, 293–300.
36 F. Benito-Lopez, R. Byrne, A. M. Raduta, N. E. Vrana, G. McGuinness and D. Diamond, *Lab Chip*, 2010, **10**, 195–201.

